



Optimum temporal and spectral window for monitoring crop marks over archaeological remains in the Mediterranean region

Athos Agapiou^{a,*}, Diofantos G. Hadjimitsis^a, Apostolos Sarris^b, Andreas Georgopoulos^c,
Dimitrios D. Alexakis^a

^a Laboratory of Geophysical-Satellite Remote Sensing & Archaeo-environment, Institute for Mediterranean Studies, Foundation for Research & Technology, Hellas (F.O.R.T.H.), Greece

^b Department of Civil Engineering and Geomatics, Faculty of Engineering and Technology, Cyprus University of Technology, 2-6, Saripolou Str., 3603 Limassol, Cyprus

^c Laboratory of Photogrammetry, School of Rural & Surveying Engineering, NTUA, Greece

ARTICLE INFO

Article history:

Received 3 July 2012

Received in revised form

4 October 2012

Accepted 22 October 2012

Keywords:

Remote sensing archaeology

Crop marks

Detection of archaeological remains

Best phenophase

Archaeological index

ABSTRACT

This paper aims to explore the formation of crop marks over archaeological features using remote sensing data. Crop marks are very important to archaeological research since they can reveal in an indirect way buried archaeological remains. Several researches have been able to locate subsurface relics via interpretation of multispectral and hyperspectral satellite images. However the best phenophase (time-window) where these crop marks are enhanced and which spectral bands are the most capable for this enhancement are still an open question for the scientific community. This study aims to address these fundamental aspects of Remote Sensing Archaeology. For this reason an extensive dataset was used: two control archaeological sites were constructed in two different areas of Cyprus (Alampra and Acheleia). In these areas both barley and wheat, were cultivated. In situ spectroradiometric measurements were taken over a whole phenological cycle (2001–2012) for both areas. More than 30 in situ campaigns were performed and more than 2600 ground measurements were collected. The phenological analysis of these measurements have shown that a period of only 15 days is best suitable for monitoring crop marks which is connected with one phenological stage; during the beginning of the boot stage of the crops. This period can be used in areas having similar climatic condition as Cyprus (Mediterranean region). Also as it was found, this phenological stage of crops might be also influenced by the climatic conditions of the area. The evaluation of a proposed Archaeological Index was performed at the Thessalian plain (central Greece), where several Neolithic settlements are established. The evaluation was made using both Hyperion and Landsat images. The results have shown that the proposed Archaeological Index is suitable for the enhancement of crop marks in satellite imagery.

© 2012 Elsevier Ltd. All rights reserved.

1. Introduction

1.1. Remote Sensing Archaeology

Satellite remote sensing in archaeology has been effectively applied since the first images have become available to archaeologists and researchers. Indeed since the second half of last century, satellite images have been largely employed in archaeological research giving a relevant contribution in the study of partially known sites or in the exploration of completely unknown

archaeological deposits (Lasaponara and Masini, 2011; Gallo et al., 2009; Rowlands and Sarris, 2007; Masini and Lasaponara, 2007). In the last decade, the new technological achievements of space technology such as higher spatial resolution and hyperspectral data, offer new opportunities for future archaeological discoveries (Giardino, 2011).

Several researchers have been able to identify old human traces and buried archaeological remains using grayscale archive aerial and satellite images (Goossens et al., 2006; Kostka, 2002; Riley, 1987), ground spectroradiometric hyperspectral data (Agapiou et al., 2012a, 2011) and image interpretation of crop marks (Gojda and Hejzman, 2012; Aqduş et al., 2012; Kaimaris et al., 2011; Alexakis et al., 2009, 2011; Laet et al., 2007; Cavalli et al., 2007). The latest is a well established procedure in the archaeological research. Crop marks may be formed in areas where vegetation overlay near-surface archaeological remains. These features are responsible in

* corresponding author.

E-mail addresses: athos.agapiou@cut.ac.cy (A. Agapiou), d.hadjimitsis@cut.ac.cy (D.G. Hadjimitsis), asaris@ret.forthnet.gr (A. Sarris), drag@central.ntua.gr (A. Georgopoulos), dimitrios.alexakis@cut.ac.cy (D.D. Alexakis).

retaining different percentage of soil moisture compared to the rest of the crops of an area. Depending on the type of the buried archaeological features, crop vigour may be enhanced or reduced (Winton and Horne, 2010).

As Kaimaris and Patias (2012) report in their study, crop marks are caused as an indirect effect of buried structures. Several researches tend to agree that such marks are difficult to be modelled, since they constitute a complicated phenomenon. Therefore several parameters should be taken into consideration, such as the characteristics of the buried features, the burial depth of them, soil characteristics, climatic and environmental parameters, cultivation techniques, etc (Agapiou et al., 2012b, 2012c; Kaimaris and Patias, 2012; Winton and Horne, 2010; Mills and Palmer, 2007). Furthermore, moisture availability and the availability of dissolved nutrients to the crops (at crucial growing times and periods for the plant) are also important parameters that need to be considered.

Crop marks can be distinguished into two main categories: positive and negative crop marks. Positive crop marks may appear in areas where subsurface trenches exist. The cover material retains dampness, resulting in the plants growing more densely and maturing later than those in neighbouring sites. Negative crop marks appear in areas where the plants grow over the buried remains of human structures, where the soil is poor in nitrates, with no dampness and therefore it cannot help plant growth (Sharpe, 2004).

1.2. Research aims

This paper aims to address two current challenges of Remote Sensing Archaeology, related to the formation of crop marks. The first one, refers to the best period (time – window) in which such crop marks can be detected using satellite images, while the second one is focused to the best spectral regions which can be used in order to enhance the crop marks in satellite imagery.

Although, these two aspects are considered to be very important for archaeological investigations via satellite images, a very little progress has been made during the last years. This is due to the fact that several satellite sensors are available for archaeological investigations while at the same time these sensors tend to have different spectral characteristics and sensitivities (Agapiou et al., 2012b). Moreover crop marks are often observed in different

types of crops (wheat; barley; corn etc), which in their turn have different phenological cycles. Moreover, the cost of acquisition of archive or new satellite images for supporting archaeological research, the spatial resolution of the images, the time of satellite overpass etc are some further limitations to examine these considerations.

For instance, Kaimaris and Patias (2012) in their study at northern Greece, argue that the period for observation of such traces relates to the period of wheat growth which is from late March to mid-May (45 days). For cotton and corn, observations can be performed from late May until late August (more than 3 months). Sharpe (2004), reports that crop marks in England are often recorded in cereal crops especially during warm and dry summer months while Ciminale et al. (2009) mention that for the Mediterranean region, crop marks are better visible from the beginning of spring up to the half or end of May. As it is shown from the previous studies, the best time-window for monitoring crop marks using remote sensing techniques is still very general and extensive.

In addition the detection of crop marks is performed on the evaluation of existing vegetation indices, such as NDVI (Lasaponara and Masini, 2007; Masini et al., 2009). Discussion regarding which spectral regions are best suitable for archaeological investigations is still very limited (Agapiou et al., 2012c; Cavalli et al., 2007).

In order to overcome such limitations and evaluate the results of the above studies, the following approach was followed. Several ground hyperspectral measurements were acquired and analysed in two different “archaeological control areas”. Two different types of crops (barley and wheat) have been examined during a whole phenological cycle. The overall results from these extensive datasets (more than 30 in situ campaigns, more than 2600 ground spectroradiometric measurements and daily detail meteorological data) have been able to identify: (a) the best phenophase for monitoring crop marks and (b) the development and evaluation of an Archaeological Index for the enhancement of crop marks.

A complete phenological cycle of crops is shown in Fig. 1. Characteristics points from the phenological cycle are marked (A–F) while natural phenomena which can be observed in the field are also shown (in *italics*). The aim of this figure is to be used from the readers in order to easily assess the results of this study shown in the next chapters. As it is shown in Fig. 1, Point A corresponds to dry soil, just before the first winter rainfalls. Wet soil, is shown in Point

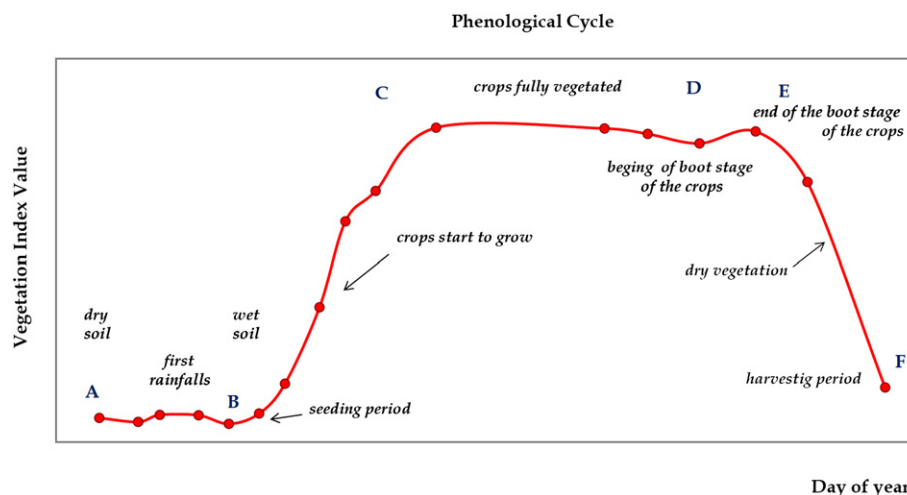


Fig. 1. Phenological cycle of crops showing the different stages of vegetation. Point A corresponds to dry soil, Point B to wet soil, Point C to the stage where the crops are fully vegetated until Point E. Point D indicates the early boot stage of the crops. Dry vegetation and harvesting period are highlighted with Points E and F respectively.

B and during the following period crops start to grow (Point B–C). During this period the crops are not fully vegetated and therefore crops do not cover the area of interest (i.e. soil background can be seen). After this short period the crops are fully vegetated (Points C–E). Point D shows the beginning of the boot stage of the crops until the end of the boot stage (Point E). Afterwards the crops begin to dry (Point E–Point F) until the harvesting period (after Point F). The length of each period can be shorten or lengthen according to the type of crop cultivated, the soil characteristics and the climatic parameters.

2. Resources and methodology

2.1. Resources

In order to monitor in a systematic basis the phenological cycle of crops, two different control fields were constructed in two different areas of Cyprus. The first area is located a few kilometers west of the Alampra village, central Cyprus (WGS 84, 36° N: 535051, 3870818) while the second one is situated in Acheleia area at the SW part of Cyprus (WGS 84, 36° N: 453112, 3843519).

In Alampra area a square 5 × 5 m was constructed in order simulate “tombs” at a depth of 25 cm. The area was then cultivated with barley crops. In Acheleia, one “control” site was constructed where local stones were placed at a depth of 25 cm below ground surface and then was cultivated with wheat crop (see Agapiou et al., 2012c, *in press*). Both areas were cultivated using traditional techniques (Fig. 2).

More than 16 in situ campaigns were performed in Alampra test field from October of 2011 until April of 2012. In Acheleia area, 17 campaigns were performed from October of 2011 until May of 2012. The measurements were performed from the sowing period until harvesting (from Point A to Point F, see Fig. 1). Ground spectroradiometric measurements were taken during the phenological cycle of barley and wheat crops, using the handheld spectroradiometer GER 1500. GER 1500 has the ability to record electromagnetic radiation from visible to near infrared spectrum (350–1050 nm) using 512 different channels.

A calibrated reference spectralon panel was used to measure the incoming solar radiation. The Lambertian spectralon panel ($\approx 100\%$ reflectance) measurement was used as reference while measurements were taken over the crops. Therefore reflectance for each measurement was calculated using the following Equation (1):

$$\text{Reflectance} = (\text{Target Radiance}/\text{Panel Radiance}) \times \text{Calibration of the panel} \quad (1)$$

In order to avoid any errors due to significant changes in the prevailing atmospheric conditions, the measurements over the panel and the target are taken in a short time (less than 2 min). In this case it is assumed that irradiance had not significant change which is true for non hazy days (Milton et al., 2009). Finally the measurements were carried out at a height of 1.2 m between 10:00 and 14:00 (local time) in order to minimize the impact of illumination changes on the spectral responses (Milton, 1987).

2.2. Methodology

The methodology followed in this study is briefly described in this section. At first, ground measurements were acquired during the phenological cycle of barley and wheat crops from the two different cases study areas. In each campaign hyperspectral measurements were taken over the “archaeological control site” (Site A) and over healthy crops from nearby the surrounding area (Site H). Then the phenological cycle of “healthy vegetation” and “archaeological site” was plotted for both crops. Statistical analysis was performed in order to compare the two samples. Then the best phenophase for both barley and wheat crop from both areas were selected and evaluated. Moreover, the impact of climate conditions was also examined.

At the same time spectral characteristics for both Site A and Site H were analyzed. Separability indices were performed in order to extract the spectral regions which can be used for the enhancement of the crop marks. The Archaeological Index, based on these spectral regions, was then evaluated in a new case study area located at the Thessalian plain (central Greece) using EO-1 Hyperion images.

3. Results

3.1. Spectral characteristics

Fig. 3 presents the reflectance values in red and near infrared (NIR) spectrum from the Alampra area. This simple diagram is the basis of the Tasseled Cap algorithm (Kauth and Thomas, 1976). The Tasseled Cap transformation is one of the available methods for enhancing spectral information content, specifically design for monitoring vegetation. As it is demonstrated in Fig. 3, after the first



Fig. 2. Alampra (left) and Acheleia (right) test fields.

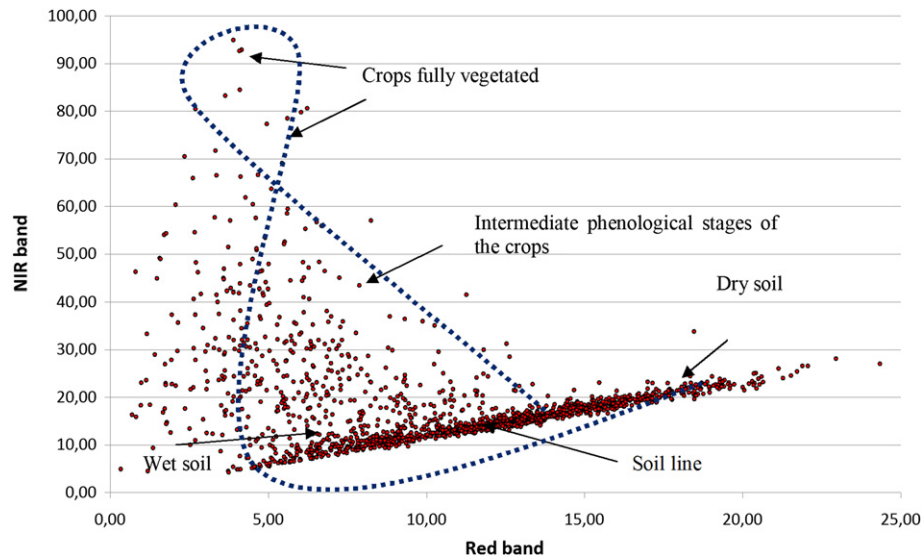


Fig. 3. Spectral signature for Band 3 and Band 4 of Landsat TM for barley crops using ground spectroradiometric measurements. Dash line indicates the normal procedure of healthy vegetation.

rainfalls in the area (moving from dry to wet soil, Point A and Point B in Fig. 1), the crops begin to grow gradually (Points B–C in Fig. 1). In this period high reflectance values of the NIR spectrum are observed due to the photosynthesis of the plant. These values are maximized when crops are fully vegetated (Points C–E in Fig. 1). Then crops are matured (yellowing colour in plants) and not photosynthetically active (Points E–F in Fig. 1). In these stages NIR values are decreasing until the harvesting period or until crops are mixed with soil.

Spectral signatures during the phenological cycle of barley and wheat crops are shown in Figs. 4 and 5. Each diagram corresponds to a different observation day for measurements taken over from both the simulated archaeological environment (Site A) and healthy areas (Site H). The phenological cycle of barley and wheat crops, in Cyprus, begins from late September to early November and lasts until mid April to early May. Such differences are occurred due to the different climatic changes and cultivation techniques performed in each area. As it is shown, before the first rainfall in the areas (Point A in Fig. 1), spectral signatures correspond to soil characteristics (Fig. 4a–e; Fig. 5a–f). Then, after the first rainfalls in each area (Fig. 4f; Fig. 5h) the crops begin to grow (Points B–C in Fig. 1). In this stage only one shoot is formed (emergence until the onset of tillering). The next stage refers to the beginning of tillering (Fig. 4f–g; Fig. 5h–g; Point C in Fig. 1) until when the tillers are formed. Then, during the next period, which last approximately 2 months, the crops are grown until the full emergence stage (Fig. 4f–k; Fig. 5g–j; Points C–E in Fig. 1). Subsequently, the head of crop is fully developed until the ripening stage which refers to the maturity or development of the grain (Fig. 4l–o; Fig. 5k–p, Point E in Fig. 1). Finally the crops are matured (Fig. 4p; Fig. 5q) and the harvesting stage is followed (Points E–F in Fig. 1).

The mean reflectance values from each campaign, over Site A (Red line) and Site H (Blue line), were calculated from 400 to 950 nm, covering both visible and NIR spectrum. Standard deviations, are also plotted in Figs. 4 and 5, and are indicated with dash lines. Special attention was given to the red and near infrared spectrum.

Meteorological data were also used in order to examine some fluctuations observed in the Acheleia area during March (Fig. 5l–n; around Point D in Fig. 1). These data were provided from the Meteorological Service of Cyprus, from a nearby

automatic meteorological station (1 km distance from the case study of Acheleia). During this period the crops were fully vegetated. As it is shown from the spectral signatures diagram, a stress condition was observed among Site A and Site H, during the in situ campaign of 21-03-2012 (Fig. 5l). However this difference is reduced a few days after (28-03-2012; Table 2: m) and then is increased the following week (03-04-2012; Fig. 5n). These variations were related to the climatic conditions of the region, and especially to the high humidity values (>70%) that were recorded on previous days (25-03-2012 until 28-03-2012) in the Acheleia area (see Fig. 6). It is therefore better to monitor crop marks when these are fully vegetated and low humidity is present in the area of interest or in days with high temperatures. In such days the crops are under stress conditions due to the procedure of photosynthesis, and therefore they are need of more water.

3.2. Phenological observations

McCloy (2010) argues that the phenological cycle of a crop can be defined as, the trace or record of the changes in a variable or attribute over the phenological period (from sowing to harvesting period). Furthermore a phenophase is referred to an observable stage or phase in the seasonal cycle of a plant that can be defined by start and end points. Data regarding the phenology of crops can be taken either from field observations or remote sensing data (Xin et al., 2002).

In order to evaluate the phenological cycle of crops from both areas, a widely used broadband index, the Normalized Difference Vegetation Index (NDVI) was used. Therefore narrow band reflectance taken from the GER 1500 spectroradiometer was recalculated according to the spectral characteristics of a specific satellite sensor. In this case ground data were converted to Landsat TM/ETM + satellite imagery based on Relative Spectral Response (RSR) filters (Fig. 7). RSR filters describe the instrument relative sensitivity to radiance at various part of the electromagnetic spectrum (Wu et al., 2010). These spectral responses have a value of 0–1 and have no units since they are relative to the peak response. Bandpass filters are used in the same way in spectroradiometers in order to transmit a certain wavelength band, and block others. The reflectance from the spectroradiometer was calculated based on

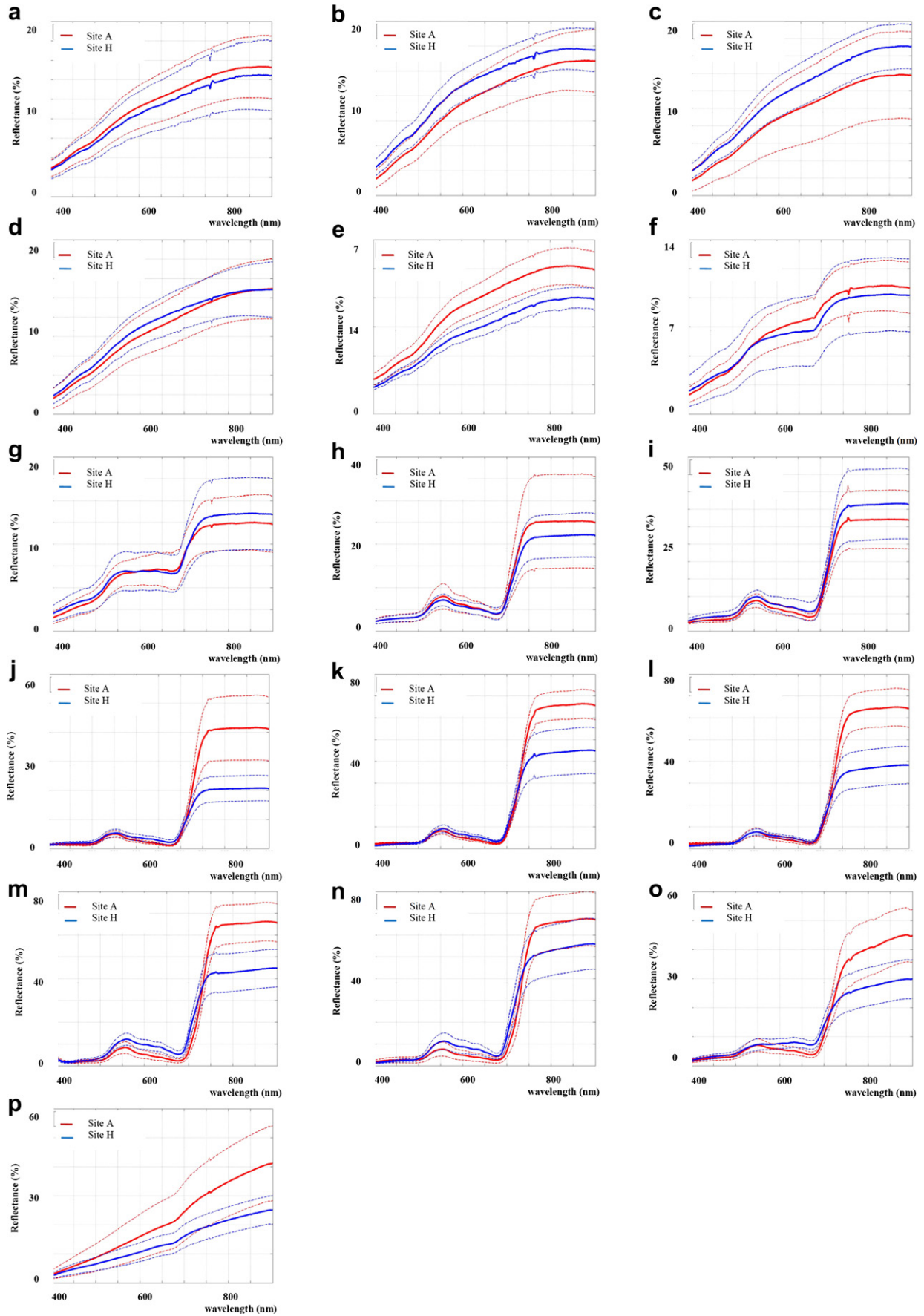


Fig. 4. Spectral signatures for barley crops (Alampra area) during the phenological cycle (a: 17-10-2011; b: 26-10-2011; c: 31-10-2011; d: 09-11-2011; e: 16-11-2011; f: 23-11-2011; g: 28-11-2011; h: 13-12-2011; i: 20-12-2011; j: 03-01-2012; k: 11-02-2012; l: 21-02-2012; m: 04-03-2012; n: 17-03-2012; o: 29-03-2012 and p: 17-04-2012).

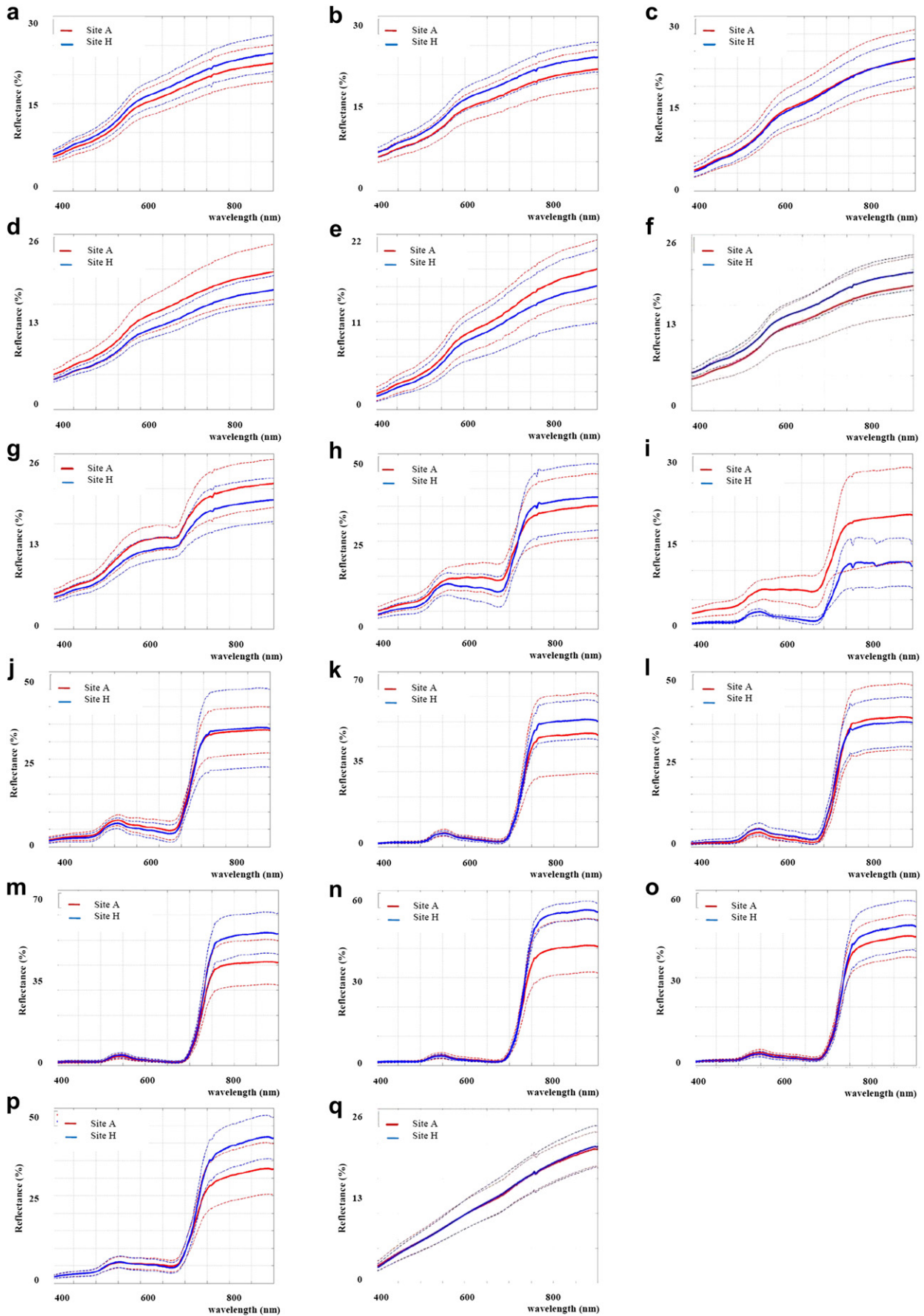


Fig. 5. Spectral signatures for wheat crops (Acheleia area) during the phenological cycle (a: 21-10-2011; b: 27-10-2011; c: 04-11-2011; d: 10-11-2011; e: 19-11-2011; f: 25-11-2011; g: 18-01-2012; h: 03-02-2012; i: 10-02-2012; j: 23-02-2012; k: 08-03-2012; l: 21-03-2012; m: 28-03-2012; n: 03-04-2012; o: 24-04-2012; p: 30-04-2012 and q: 15-05-2012).

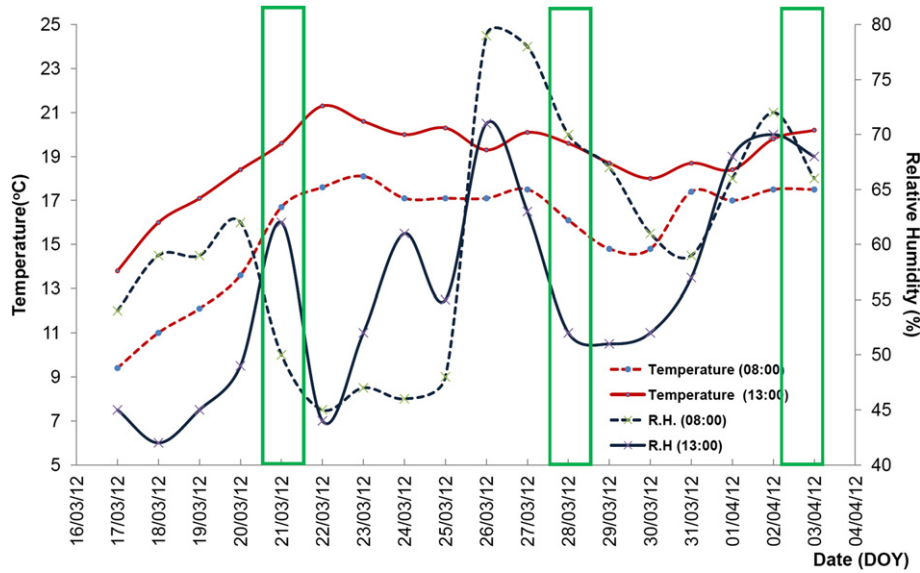


Fig. 6. Meteorological data from 17-03-2012 until 03-04-2012 recorded in the Acheleia area. The total rainfall for this period was .00 mm. Daily data were provided from the Meteorological Service of Cyprus.

the wavelength of each sensor and the RSR filter as follows (Alexakis et al., 2012):

$$R_{band} = \frac{\sum (R_i * RSR_i)}{\sum RSR_i} \quad (2)$$

Where:

- R_{band} = reflectance at a range of wavelength (e.g. Band 1)
- R_i = reflectance at a specific wavelength (e.g. R_{450 nm})
- RSR_i = Relative Response value at the specific wavelength

Vegetation indices can be used as indicators of the different phenological stages of a crop. Both theoretical analyses and field studies have shown that such indices are near-linearly related to photosynthetically active plants which absorb radiation, and therefore to light-dependent physiological processes like photosynthesis, occurring in the upper canopy (Glenn et al., 2008). The NDVI index was developed by Rouse et al. in 1974 and since then it was applied in several applications.

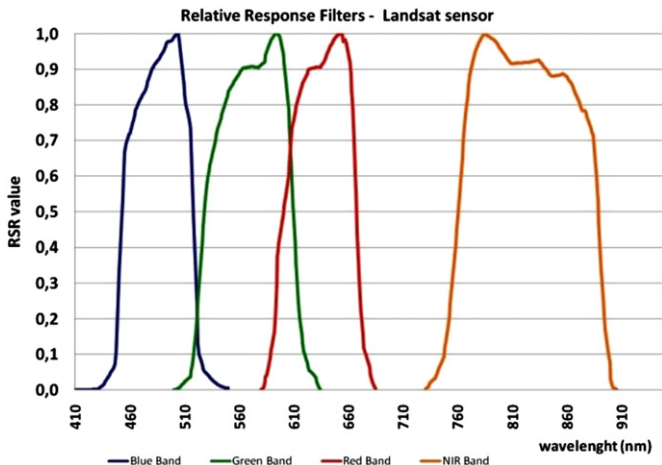


Fig. 7. Relative Response filters for Bands 1–4 of Landsat TM/ETM + sensor (Alexakis et al., 2012).

The phenological cycles for barley and wheat crops from Alampra and Acheleia area are shown in Figs. 8 and 9 respectively. In each figure two phenological cycles are presented: for Site A (“control archaeological area”) and for Site H (“healthy vegetation”). Standard deviations of the NDVI values, from each campaign are also plotted in Figs. 8 and 9. Higher standard deviations are expected during the growing period of the crops (from December to April; Points C–E in Fig. 1) due to the rapid changes of the plant. Hatfield and Prueger (2010) reported that for accurate development of vegetation indices frequent observations during the growing season are necessary in order to monitor the dynamic nature of the reflectance. After the performance of Student’s *t*-test for both areas it was found that a significant statistical difference exist for the Alampra case study (NDVI values between Site A and Site H) while for Acheleia site the statistical difference found was very closed to the theoretical statistical difference, during this period.

As it is shown in Fig. 8, the growing period of barley begins during November (DOY ≈ 330; Point B in Fig. 1). Barley crops start to grow and during January (DOY ≈ 360) the first observations of crop marks can be seen (Points B–C in Fig. 1). Indeed, crop marks can be recorded during the rest of the period until the harvesting period (DOY ≈ 460; Point B–E in Fig. 1). Similar observations are also recorded for the Acheleia site as it is shown in Fig. 9.

The results have shown that the best period for monitoring crop marks using remote sensing data is during the full emergence stage of the crops and boot stage of the plants (gray colour in Figs. 8 and 9; Points C–E in Fig. 1). During this period a significant statistical difference exist between NDVI values for Site A and Site H.

In detail as it was found, the best phenophase is around the beginning of the boot stage (Point D in Fig. 1). During this short period the difference of the NDVI index is maximized between Site A and Site H. In this way the contrast between these sites is maximized. This conclusion was compatible for both areas (Alampra and Acheleia), even though many differences are recorded from these sites: different types of crops, different soil characteristics, cultivations techniques and climate conditions. Based from this analysis the best phenophase for monitoring crop marks is limited to approximately 15 days. This short period corresponds to the natural time-window needed by the crops in order to begin the boot stage.

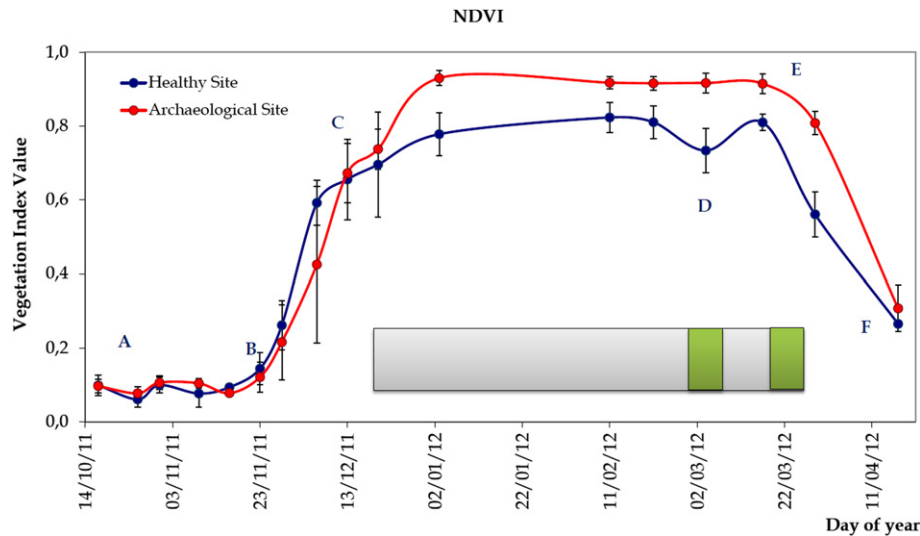


Fig. 8. The phenological cycle of barley crops at Alampra area. The overall period where observations of crop marks can be performed is indicated in the grey region, while the best phenophase where the difference of crop marks is maximized is shown in the green region. (For interpretation of the references to colour in this figure legend, the reader is referred to the web version of this article.)

3.3. Archaeological Index

3.3.1. Development of the Archaeological Index

The development of an Archaeological Index aims to enhance crop marks which are related to buried archaeological remains, as they are recorded from multispectral/hyperspectral remote sensing images. For this reason spectral regions which are capable to distinguish the spectral diversity of vegetation due to archaeological remains were examined. Three main separability indices were evaluated: (a) Euclidean distance, (b) Mahalanobis distance and (c) Cosine similarity, in the context of this study, in order to examine the separability of reflectance values from “healthy vegetation” (Site H) and “archaeological areas” (Site A). The first method simply calculates the Euclidean distance between a pair of observations (i.e. healthy site and archaeological site) (Hastie and Tibshirani, 1996) while the Mahalanobis distance exploits the covariance

matrix of the measurements (De Maesschalck et al., 2000). Finally the Cosine similarity refers to the similarity between two vectors by calculating the Cosine of the angle formed by these vectors (Kruse et al., 1993).

The whole dataset from the two study areas (barley and wheat crops) was analysed separately and the final outcome came to similar conclusions regarding the spectral regions where spectral enhancement is maximized. In this section, the final outcome of this analysis is presented (for further details see Agapiou et al., 2012c). Euclidean distance results are shown in Table 1, Mahalanobis distance result are shown in Table 2 while in Table 3 the Cosine similarity results are presented.

Based on analysis of separability indices, it was found that multispectral sensors which are sensitive to near infrared wavelengths are very promising in recording crop reflectance variations due to buried archaeological remains. This observation is widely

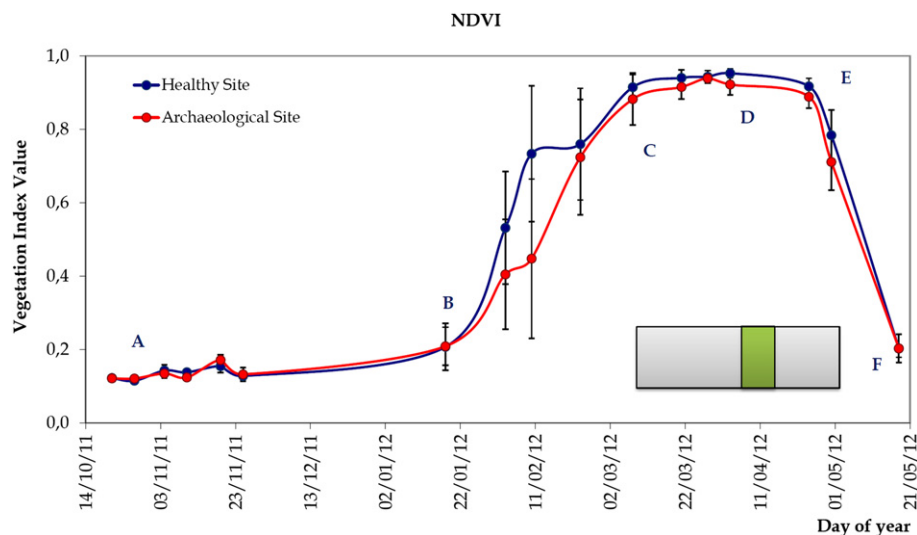


Fig. 9. The phenological cycle of barley crops at Acheleia area. In gray is shown the overall period where observations of crop marks can be performed is indicated in the grey region, while in green the best phenophase where the difference of crop marks is maximized is shown in the green region. (For interpretation of the references to colour in this figure legend, the reader is referred to the web version of this article.)

Table 1

Separability results for Alampra case study using the Euclidean distance algorithm (Agapiou et al., 2012c).

Wavelength (nm)	450	500	550	600	650	700	750	800	850	900
450	.000									
500	1.464	.000								
550	6.021	4.557	.000							
600	5.964	4.500	.107	.000						
650	5.845	4.381	.178	.132	.000					
700	9.444	7.980	3.424	3.480	3.599	.000				
750	27.942	26.493	22.000	22.073	22.178	18.673	.000			
800	30.951	29.508	25.034	25.109	25.212	21.728	3.089	.000		
850	31.885	30.442	25.966	26.042	26.145	22.656	4.000	.936	.000	
900	32.107	30.663	26.184	26.259	26.362	22.870	4.205	1.166	.246	.000

Table 2

Separability results for Alampra case study using the Mahalanobis distance algorithm (Agapiou et al., 2012c).

Wavelength (nm)	450	500	550	600	650	700	750	800	850	900
450	.000									
500	.458	.000								
550	1.890	1.431	.000							
600	2.011	1.553	.126	.000						
650	1.879	1.421	.016	.133	.000					
700	3.160	2.702	1.271	1.149	1.281	.000				
750	2.941	2.572	1.727	1.728	1.742	1.833	.000			
800	2.609	2.368	2.140	2.199	2.150	2.704	1.026	.000		
850	2.715	2.463	2.170	2.223	2.181	2.675	.950	.124	.000	
900	2.808	2.533	2.129	2.172	2.141	2.552	.786	.298	.185	.000

Table 3

Separability results for Alampra case study using the Cosine similarity algorithm (Agapiou et al., 2012c).

Wavelength (nm)	450	500	550	600	650	700	750	800	850	900
450	.0000									
500	.0000	.0000								
550	.0001	.0000	.0000							
600	.0001	.0000	.0000	.0000						
650	.0002	.0001	.0000	.0000	.0000					
700	.0000	.0000	.0001	.0001	.0002	.0000				
750	.0119	.0108	.0101	.0103	.0093	.0123	.0000			
800	.0162	.0149	.0141	.0143	.0131	.0166	.0003	.0000		
850	.0141	.0129	.0121	.0123	.0112	.0145	.0001	.0001	.0000	
900	.0162	.0149	.0141	.0143	.0131	.0166	.0003	.0000	.0001	.0000

known and applied in vegetation studies using the VNIR part of the spectrum. However in this case, using the ground hyperspectral data, a detail analysis was able to be performed. Indeed, based on the results from Tables 1–3 for the Alampra case study, and the hyperspectral measurements from the Acheleia area (not shown here) have shown that spectral regions around 700 nm–800 nm (near infrared and red edge) are very promising for the detection of crop marks. As it is shown in Tables 1–3, these spectral regions had the highest separability. Similar results were found for Acheleia study also (see Agapiou et al., 2012c). High separability values were also recorded and for the VNIR and blue part of the spectrum. However, the use of the blue part of the spectrum could be found very problematic for satellite images due to the Rayleigh scattering phenomenon. Therefore the Archaeological Index could follow the following function:

$$A.I. = f(p_{800}, p_{700}) \quad (3)$$

Where

A.I.: Archaeological Index
 p_{800} : reflectance at 800 nm
 p_{700} : reflectance at 700 nm

3.3.2. Sensitivity of the Archaeological Index

In order to quantify the enhancement of the proposed Archaeological Index, a statistical analysis was contacted. The detection of crop marks is performed through the visual difference of vegetation above the subsurface residues in relation to the surroundings of this area. Thus, this difference can be expressed using the following equation:

$$\text{Sensitivity} = \left| \frac{\text{Value crop marks} - \text{Value healthy crops}}{\text{Value healthy crops}} \right| * 100 \quad (4)$$

Where:

Sensitivity: the % difference between crop marks and surrounding area
 Value crop marks: value of the vegetation index at the area of crop marks
 Value healthy crops: value of the vegetation index at the surrounding area

Sensitivity of the normalized Archaeological Index was made for both areas of Alampra and Acheleia, during the vegetation growth

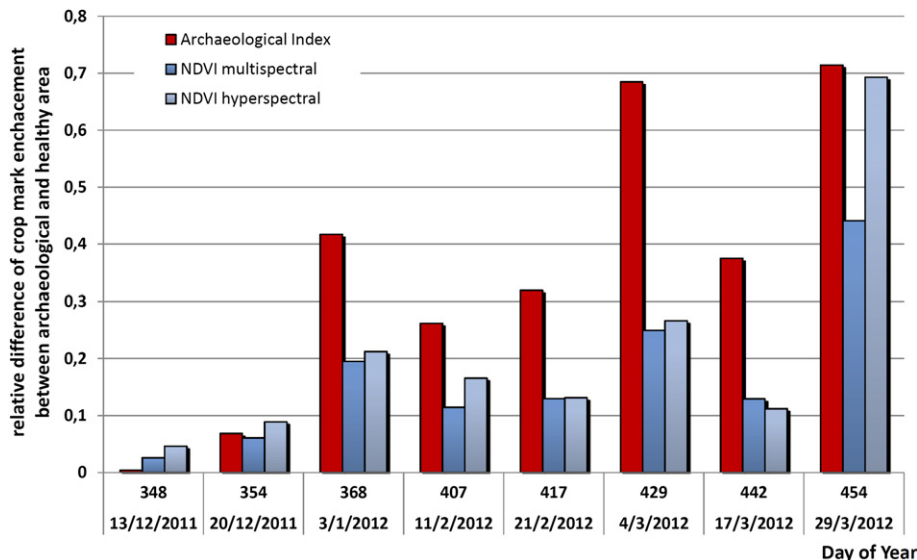


Fig. 10. Relative difference between crop marks and healthy areas based from the Alampra test field, for the proposed Archaeological Index, NDVI multispectral and NDVI hyperspectral.

period (December to April, Points C–E in Fig. 1). During this period the area is fully vegetated and therefore soil background noise is minimized. The results were directly compared to the $NDVI_{(multispectral)}$ and $NDVI_{(hyperspectral)}$ (see Equations (5)–(7)).

Normalized Archaeological Index

$$= (p_{800} - p_{700}) / (p_{800} + p_{700}) \tag{5}$$

$$NDVI_{(multispectral)} = (p_{VNIR} - p_{RED}) / (p_{VNIR} + p_{RED}) \tag{6}$$

$$NDVI_{(hyperspectral)} = (p_{800} - p_{670}) / (p_{800} + p_{670}) \tag{7}$$

Where:

p_{800} : reflectance at 800 nm
 p_{700} : reflectance at 700 nm

p_{670} : reflectance at 670 nm
 p_{RED} : reflectance at red part of the spectrum (630–690 nm)
 p_{VNIR} : reflectance at VNIR part of the spectrum (760–900 nm)

The final results area shown in Fig. 10 and Fig. 11. These diagrams indicate the relative difference of each index as recorded over the crop marks in comparison to healthy vegetation. As it shown all three indices can be used for crop marks' observations. However, the normalized Archaeological Index can distinguish crop marks from the surrounding area in a more sufficient way. Indeed, as it is indicated in Fig. 10, for barley crops, the normalized Archaeological Index enhanced the final results more than the other two widely used indices. During the beginning of the boot stage (when this enhancement is maximized – see Chapter 3.2), the difference is more than 100% compared to other indices (Point D in Fig. 1). Similar results were recorded for the Acheleia area also (Fig. 11).

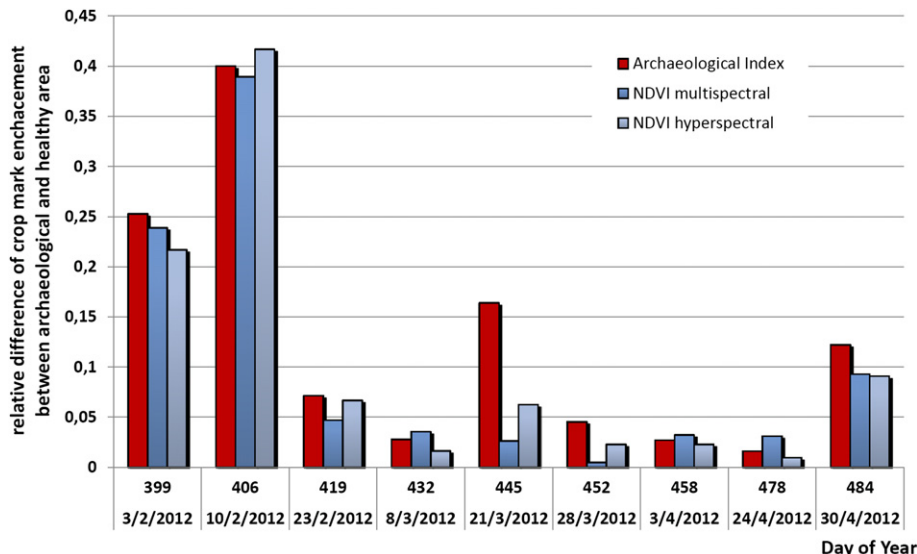


Fig. 11. Relative difference between crop marks and healthy areas based from the Acheleia test field, for the proposed Archaeological Index, NDVI multispectral and NDVI hyperspectral.

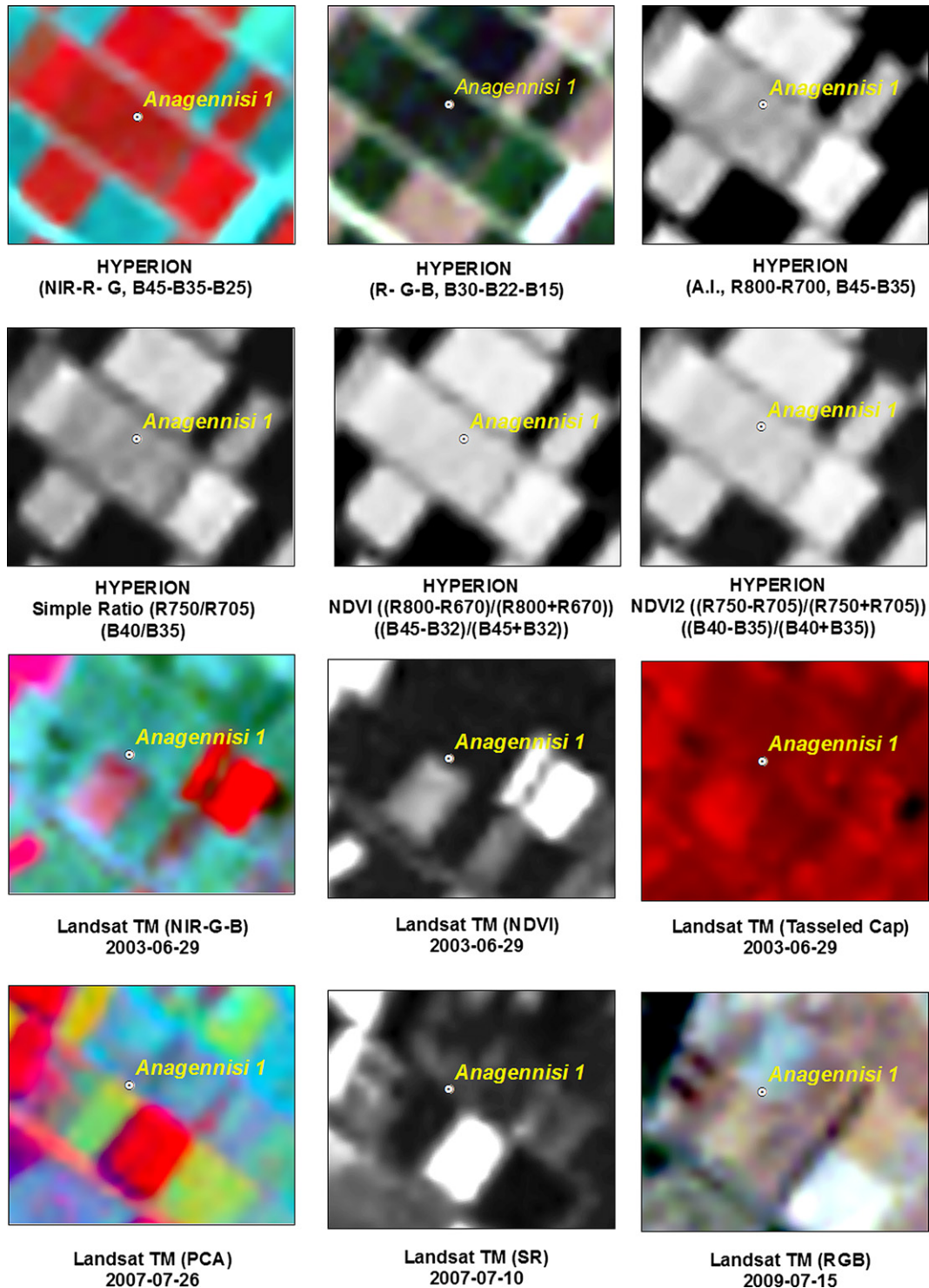


Fig. 12. Results of the hyperspectral image of Hyperion (03-09-2001) and Landsat TM (29-06-2003/10-07-2007/26-07-2007/15-07-2009), for the archaeological site "Anagennisi 1". The application of the Archaeological Index is shown in 1st row, 3rd column. The date and the algorithm used for each image is mentioned below of the each image.

3.3.3. Evaluation of Archaeological Index

Having taken into account the observations of the two different phenological cycles of barley and wheat crops, the Archaeological Index was evaluated in terms of interpretation using hyperspectral images (EO-1, Hyperion sensor). The case study area of this application was the Thessalian plain, located in central Greece. In this area several Neolithic settlements are established in the form of tells called "magoules" (see Agapiou et al., 2012a).

In Figs. 12 and 13, the results of this evaluation are presented. Besides Hyperion images, several other multispectral Landsat TM/ETM+ images were used. Further to the Archaeological Index, other image analysis techniques were also applied to the satellite images. In detail, a true colour composite (R-G-B) was constructed for Landsat images, along with the NIR-R-G composite for both set of images (Hyperion and Landsat). Additionally the $NDVI_{\text{multispectral}}$ (see Equation (6)) and $NDVI_{\text{hyperspectral}}$ (see Equation (7)) were also

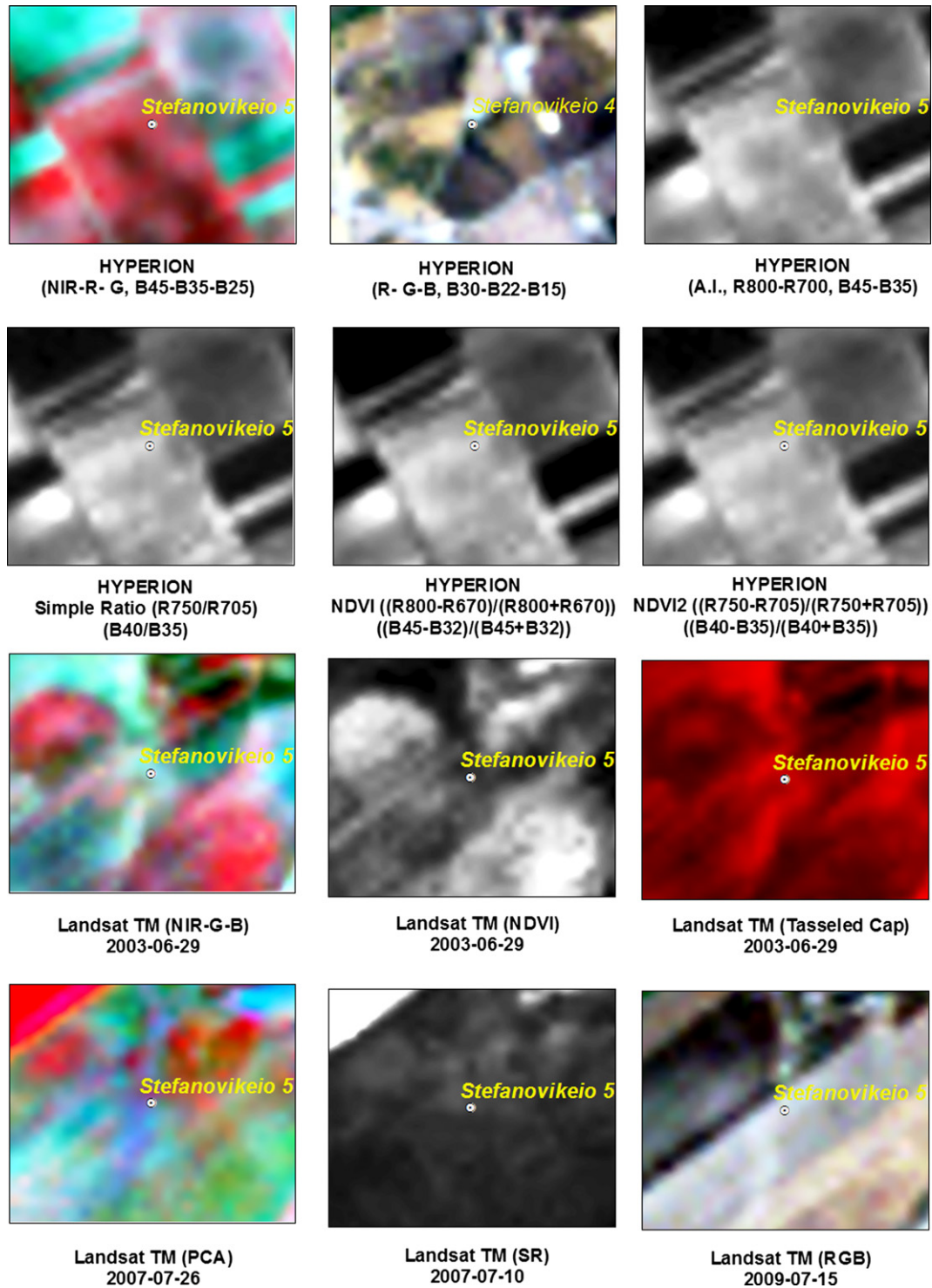


Fig. 13. Results of the hyperspectral image of Hyperion (19-09-2001) and Landsat TM (29-06-2003/10-07-2007/26-07-2007/15-07-2009), for the archaeological site "Stefanovikeio 5". The application of the Archaeological Index is shown in 1st row, 3rd column. The date and the algorithm used for each image is mentioned below of the each image.

evaluated. Simple Ratio (SR) index which uses the characteristic curve of vegetation canopies at the red and near infrared spectrum (red edge) was applied. Finally Tasseled Cap images and Principal Component Analysis (PCA) were tested.

Figs. 12–13 depicted that the proposed Archaeological Index distinguishes the Neolithic tells of "Anagennisi" and "Stefanovikeio 5", in contrast to any other analysis. Each tell's crop mark was

enhanced after the application of the Archaeological Index and the trace of both tells was highlighted. In contrast, concerning the application of the rest of techniques, the Neolithic tells were not clearly visible and they were difficult to be distinguished from the surrounding cultivated area. Indeed a circular crop mark was visible for both areas using the Archaeological Index while in several other indices and algorithm applied these crop marks could not be

recognized. Several Landsat images were analysed in order to examine if the tells were able to be detected in different periods, without any result.

As it was found, Hyperion hyperspectral images can better enhance the final outcome in contrast to the multispectral Landsat images, having the same spatial resolution (30 m). The analysis performed (PCA, Tasseled Cap) to the latest dataset of Landsat concluded to very poor results. Indeed, the poor results of Landsat imagery concerning Thessalian plain archaeological investigations have been also reported in previous studies (Alexakis, 2009). It should be noticed that similar radiometric enhancements were performed for all images.

In order to quantify the contrast between crop marks of the magoules and the surrounding area a direct comparison was made for the different algorithms applied to the above images. For this reason several measurements from the images were made both in the top of the magoula and the surrounding area. The results have shown that the proposed Archaeological Index was able to distinguish better the magoules, with a relative contrast of 27% and 60% compare to the “Anagennisi” and “Stefanovikeio 5” surrounding area, respectively. Similarly, Simple Ratio’s contrast was estimated at 14% and 18%, while the $NDVI_{\text{hyperspectral}}$ was calculated to 8% and 44%. Finally the relative contrast for $NDVI_2_{\text{hyperspectral}}$ index was estimated at 11% and 33%. These results are also compatible with visual interpretation.

Concerning the Landsat images these were not examined since their interpretation was found very poor and very difficult to recognize and traces from the magoules. Indeed as it is shown both in Figs. 12 and 13 the detection of the “Anagennisi” and “Stefanovikeio 5” is not an easy task.

4. Conclusions

This paper aimed to investigate two scientific challenges of Remote Sensing Archaeology. The first one is related to the identification of the best period for monitoring crop marks while the second one is focused to the identification of the best spectral regions for enhancing crop marks in satellite imagery. For the aims of this study several ground measurements were taken and analysed. Spectral signature profiles for the whole phenological cycle of barley and wheat crops were evaluated.

The phenological cycles, for both barley and wheat crops, have shown that the best period for monitoring crop marks is during the beginning of the crops boot stage (Point D in Fig. 1). This period is limited to only 15 days. In this way the authors have successfully connect the best phenophase (time-window) with a unique phenological stage of the crop. This phenological stage can be further examined in other environments as well (i.e. non Mediterranean region). Indeed, according to the results this period is suitable for the detection of crop marks, regardless the type of vegetation and soil conditions. This is very important for future archaeological investigations since satellites can be scheduled to cover an archaeological area during this short period. In this period crop marks are expected to be enhanced. In addition, researchers can use archive imagery of this period in order to trace crop marks of under investigation areas. This conclusion is not opposed to previous reports regarding the best period for monitoring crop marks. In contrast it provides a more narrow time-window regardless the type of the crop, soil conditions, cultivation techniques etc. Moreover, the meteorological records have proved that if any stress climatic conditions are observed in an area they may enhance the final result or the opposite regarding non stress climatic conditions.

Finally, separability analysis has shown that spectral regions around the red edge and NIR spectrum (700 and 800 nm respectively) are able to distinguish crop marks. The above conclusion was

evaluated successfully at the Thessalian plain, for the detection of Neolithic tells, using Hyperion images. The results of the application of the proposed Archaeological Index were evaluated with other techniques such as colour composites, vegetation indices, PCA, Tasseled Cap etc.

Both conclusions from the current analyses performed in this paper, are expected to be further evaluated in the archaeological sites, using different types of crops and satellite images. Although the case study concerns the Mediterranean region it should be noticed that the overall methodology could be implemented worldwide and provide significant results for detection of crop marks.

Acknowledgments

The results are part of the PhD dissertation of Mr. Athos Agapiou. The authors would like to express their appreciation to the Alexander Onassis Foundation for funding the PhD study. Also thanks are given to the Remote Sensing Laboratory of the Department of Civil Engineering & Geomatics at the Cyprus University of Technology for the support (<http://www.cut.ac.cy/>).

Appendix A. Supplementary data

Supplementary data related to this article can be found at <http://dx.doi.org/10.1016/j.jas.2012.10.036>.

References

- Agapiou, A., Hadjimitsis, G.D., 2011. Vegetation indices and field spectroradiometric measurements for validation of buried architectural remains: verification under area surveyed with geophysical campaigns. *Journal of Applied Remote Sensing* 5, 053554. <http://dx.doi.org/10.1117/1.3645590>.
- Agapiou, A., Hadjimitsis, G.D., Alexakis, D., Sarris, A., 2012a. Observatory validation of Neolithic tells (“Magoules”) in the Thessalian plain, central Greece, using hyperspectral spectroradiometric data. *Journal of Archaeological Science*. ISSN: 0305-4403 39 (5). ISSN: 0305-4403, 1499–1512. <http://dx.doi.org/10.1016/j.jas.2012.01.001>.
- Agapiou, A., Alexakis, D.D., Hadjimitsis, G.D., 2012b. Spectral sensitivity of ALOS, ASTER, IKONOS, LANDSAT and SPOT satellite imagery intended for the detection of archaeological crop marks. *International Journal of Digital Earth*, 1–22. <http://dx.doi.org/10.1080/17538947.2012.674159>.
- Agapiou, A., Hadjimitsis, G.D., Georgopoulos, A., Sarris, A., Alexakis, D.D., 2012c. Towards an archaeological index: identification of the spectral regions of stress vegetation due to buried archaeological remains. In: Ioannides, M., et al. (Eds.), *Lecture Notes of Computer Science*. Springer, Heidelberg, pp. 129–138. EuroMed 2012, 7616.
- Agapiou, A., Hadjimitsis, G.D., Sarris, A., Georgopoulos, A. A new method for the detection validation of architectural remains using field spectroscopy: experimental remote sensing archaeology. In: *Proceedings XVI Congress of the UISPP (International Union for Prehistoric and Protohistoric Sciences)*, 4–10 September, Florianopolis, Brazil, in press.
- Alexakis, D., Sarris, A., Astaras, T., Albanakis, K., 2009. Detection of Neolithic settlements in Thessaly (Greece) through multispectral and hyperspectral satellite imagery. *Sensors* 9, 1167–1187.
- Alexakis, D., Sarris, A., Astaras, T., Albanakis, K., 2011. Integrated GIS, remote sensing and geomorphologic approaches for the reconstruction of the landscape habitation of Thessaly during the Neolithic period. *Journal of Archaeological Science* 38, 89–100.
- Alexakis, D.D., Agapiou, A., Hadjimitsis, G.D., Sarris, A., 2012. Remote sensing applications in archaeological research. In: Escalante-Ramirez, Boris (Ed.), *Remote Sensing – Applications*, ISBN 978-953-51-0651-7. InTech, Available from: <http://www.intechopen.com/books/remote-sensing-applications/remote-sensing-applications-in-archaeology>.
- Alexakis, D., 2009. *The Contribution of Geomorphology Using Satellite Remote Sensing and Geographical Information Systems for Mapping Archaeological Sites*. PhD dissertation (in Greek). Aristotle University of Thessaloniki, Faculty of Sciences, School of Science.
- Aqdu, S.A., Hanson, S.W., Drummond, J., 2012. The potential of hyperspectral and multi-spectral imagery to enhance archaeological cropmark detection: a comparative study. *Journal of Archaeological Science*. ISSN: 0305-4403 39 (7). ISSN: 0305-4403, 1915–1924. <http://dx.doi.org/10.1016/j.jas.2012.01.034>.
- Cavalli, R.S., Colosi, F., Palombo, A., Pignatti, S., Poscolieri, M., 2007. Remote hyperspectral imagery as a support to archaeological prospection. *Journal of Cultural Heritage* 8, 272–283.

- Ciminale, M., Gallo, D., Lasaponara, R., Masini, N., 2009. A multiscale approach for reconstructing archaeological landscapes: applications in northern Apulia (Italy). *Archaeological Prospection* 16, 143–153. <http://dx.doi.org/10.1002/arp.356>.
- De Maesschalck, R., Jouan-Rimbaud, D., Massart, D.L., 2000. The Mahalanobis distance. *Chemometrics and Intelligent Laboratory Systems*. ISSN: 0169-7439 50 (1–4). ISSN: 0169-7439, 1–18. [http://dx.doi.org/10.1016/S0169-7439\(99\)00047-7](http://dx.doi.org/10.1016/S0169-7439(99)00047-7).
- Gallo, D., Ciminale, M., Becker, H., Masini, N., 2009. Remote sensing techniques for reconstructing a vast Neolithic settlement in Southern Italy. *Journal of Archaeological Science*. ISSN: 0305-4403 36 (1). ISSN: 0305-4403, 43–50. <http://dx.doi.org/10.1016/j.jas.2008.07.002>.
- Giardino, J.M., 2011. A history of NASA remote sensing contributions to archaeology. *Journal of Archaeological Science*. ISSN: 0305-4403 38 (9). ISSN: 0305-4403, 2003–2009. <http://dx.doi.org/10.1016/j.jas.2010.09.017>.
- Glenn, E.P., Huete, A.R., Nagler, P.L., Nelson, S.G., 2008. Relationship between remotely-sensed vegetation indices, canopy attributes and plant physiological processes: what vegetation indices can and cannot tell us about the landscape. *Sensors* 8, 2136–2160.
- Gojda, M., Hejcman, M., 2012. Cropmarks in main field crops enable the identification of a wide spectrum of buried features on archaeological sites in Central Europe. *Journal of Archaeological Science*. ISSN: 0305-4403 39 (6). ISSN: 0305-4403, 1655–1664. <http://dx.doi.org/10.1016/j.jas.2012.01.023>.
- Goossens, R., Wulf, De A., Bourgeois, J., Gheyle, W., Willems, T., 2006. Satellite imagery and archaeology: the example of CORONA in the Altai Mountains. *Journal of Archaeological Science*. ISSN: 0305-4403 33 (6). ISSN: 0305-4403, 745–755. <http://dx.doi.org/10.1016/j.jas.2005.10.010>.
- Hastie, T., Tibshirani, R., 1996. Discriminant adaptive nearest neighbor classification. *IEEE Transactions on Pattern Analysis and Machine Intelligence* 18 (6), 607–615. 96.
- Hatfield, J.L., Prueger, J.H., 2010. Value of using different vegetative indices to quantify agricultural crop characteristics at different growth stages under varying management practices. *Remote Sensing* 2, 562–578. <http://dx.doi.org/10.3390/rs2020562>.
- Kaimaris, D., Patias, P., 2012. Best period for high spatial resolution satellite images for the detection of marks of buried structures. *The Egyptian Journal of Remote Sensing and Space Science*. ISSN: 1110-9823 ISSN: 1110-9823. <http://dx.doi.org/10.1016/j.ejrs.2011.12.001>.
- Kaimaris, D., Georgoula, O., Patias, P., Stylianidis, E., 2011. Comparative analysis on the archaeological content of imagery from Google Earth. *Journal of Cultural Heritage*. ISSN: 1296-2074 12 (3). ISSN: 1296-2074, 263–269. <http://dx.doi.org/10.1016/j.culher.2010.12.007>.
- Kauth, J.R., Thomas, S.G., 1976. The tasseled Cap – a graphic description of the spectral-temporal development of agricultural crops as seen by landsat. In: *Proceeding Symposium on Machine Processing of Remotely Sensed Data*, Purdue University of West Lafayette, Indiana, 1976, 4B, pp. 44–51.
- Kostka, R., 2002. The world mountain Damavand: documentation and monitoring of human activities using remote sensing data. *ISPRS Journal of Photogrammetry and Remote Sensing*. ISSN: 0924-2716 57 (1–2). ISSN: 0924-2716, 5–12. [http://dx.doi.org/10.1016/S0924-2716\(02\)00116-8](http://dx.doi.org/10.1016/S0924-2716(02)00116-8).
- Kruse, F.A., Lefkoff, A.B., Boardman, J.B., Heidebrecht, K.B., Shapiro, A.T., Barloon, P.J., Goetz, A.F.H., 1993. The spectral image processing system (SIPS) – interactive visualization and analysis of imaging spectrometer data. *Remote Sensing of the Environment* 44, 145–163.
- Laet, V., Paulissen, E., Waelkens, M., 2007. Methods for the extraction of archaeological features from very high-resolution Ikonos-2 remote sensing imagery, Hisar (southwest Turkey). *Journal of Archaeological Science* 34, 830–841.
- Lasaponara, R., Masini, N., 2007. Detection of archaeological crop marks by using satellite QuickBird multispectral imagery. *Journal of Archaeological Science*. ISSN: 0305-4403 34 (2). ISSN: 0305-4403, 214–221. <http://dx.doi.org/10.1016/j.jas.2006.04.014>.
- Lasaponara, R., Masini, N., 2011. Satellite remote sensing in archaeology: past, present and future perspectives. *Journal of Archaeological Science*. ISSN: 0305-4403 38 (9). ISSN: 0305-4403, 1995–2002. <http://dx.doi.org/10.1016/j.jas.2011.02.002>.
- Masini, N., Lasaponara, R., 2007. Investigating the spectral capability of QuickBird data to detect archaeological remains buried under vegetated and not vegetated areas. *Journal of Cultural Heritage*. ISSN: 1296-2074 8 (1). ISSN: 1296-2074, 53–60. <http://dx.doi.org/10.1016/j.culher.2006.06.006>.
- Masini, N., Lasaponara, R., Orefici, G., 2009. Addressing the challenge of detecting archaeological adobe structures in Southern Peru using QuickBird imagery. *Journal of Cultural Heritage*. ISSN: 1296-2074 10 (1). ISSN: 1296-2074, e3–e9. <http://dx.doi.org/10.1016/j.culher.2009.10.005>.
- McCloy, K.R., 2010. Development and evaluation of phenological change indices derived from time series of image data. *Remote Sensing* 2, 2442–2473.
- Mills, J., Palmer, R., 2007. Populating Clay Landscapes. Tempus, Stroud.
- Milton, E.J., Schaeppman, M.E., Anderson, K., Kneubühler, M., Fox, N., 2009. Progress in field spectroscopy. *Remote Sensing of Environment* 113, 92–109.
- Milton, E.J., 1987. Principles of field spectroscopy. *Remote Sensing of Environment* 8 (12), 1807–1827.
- Riley, D.N., 1987. *Air Photography and Archaeology*. Duckworth, London.
- Rouse, J.W., Haas, R.H., Schell, J.A., Deering, D. W., Harlan, J.C., 1974. *Monitoring the Vernal Advancements and Retrogradation (Greenwave Effect) of Nature Vegetation*. NASA/GSFC Final Report, Greenbelt.
- Rowlands, A., Sarris, A., 2007. Detection of exposed and subsurface archaeological remains using multi-sensor remote sensing. *Journal of Archaeological Science* 34 (5), 795–803.
- Sharpe, L., 2004. *Geophysical, Geochemical and Arable Crop Responses to Archaeological Sites in the Upper Clyde Valley, Scotland*. PhD thesis, University of Glasgow.
- Winton, H., Horne, P., 2010. National archives for national survey programmes: NMP and the English heritage aerial photograph collection. In: *Landscapes Through the Lens: Aerial Photographs and Historic Environment*. Aerial Archaeology Research Group No. 2, pp. 7–18.
- Wu, X., Sullivan, T.J., Heidinger, K.A., 2010. Operational calibration of the advanced very high resolution radiometer (AVHRR) visible and near-infrared channels. *Canadian Journal of Remote Sensing* 36 (5), 602–616.
- Xin, J., Yu, Z., Leeuwen van, L., Driessen, M.P., 2002. Mapping crop key phenological stages in the North China Plain using NOAA time series images. *International Journal of Applied Earth Observation and Geoinformation*. ISSN: 0303-2434 4 (2). ISSN: 0303-2434, 109–117. [http://dx.doi.org/10.1016/S0303-2434\(02\)00007-7](http://dx.doi.org/10.1016/S0303-2434(02)00007-7).